Available online at www.sciencedirect.com
SCIENCE DIRECT
Journal of Power Sources 157 (2006) 471–476
JOURNAL OF POWER SOURCES
www.elsevier.com/locate/jpowsour

Li^+ ion diffusion in $LiMn_2O_4$ thin film prepared by PVP sol–gel method

Young Ho Rho [a,1], Kaoru Dokko [a,b], Kiyoshi Kanamura [a,b,*]

[a] *Department of Applied Chemistry, Graduate School of Engineering, Tokyo Metropolitan University, 1-1 Minami-Ohsawa, Hachioji, Tokyo 192-0397, Japan*
[b] *CREST, Japan Science and Technology Agency, 4-1-8 Honcho, Kawaguchi, Saitama 332-0012, Japan*

Received 18 July 2005; received in revised form 21 July 2005; accepted 21 July 2005
Available online 30 August 2005

Abstract

$LiMn_2O_4$ thin film (1 μm thick) was prepared on a gold substrate by the PVP sol–gel method. The electrochemical properties of the thin-film electrode were studied in an electrolyte 1 mol dm^{-3} $LiClO_4$/(ethylene carbonate + diethyl carbonate). The prepared $LiMn_2O_4$ showed a good charge–discharge performance, and the capacity fade was ca. 20% during 200 cycles. The Li^+ ion diffusion in the $LiMn_2O_4$ thin film was investigated by means of potentiostatic intermittent titration technique and electrochemical impedance spectroscopy. The chemical diffusion coefficients were estimated to be 10^{-8} to 10^{-10} cm^2 s^{-1}.

Keywords: $LiMn_2O_4$; Sol–gel; Thin-film electrode; Rechargeable lithium batteries; Diffusion coefficient

1. Introduction

Typical cathode materials for rechargeable lithium batteries, such as $LiCoO_2$ and $LiMn_2O_4$, have been investigated by many researchers [1–5]. $LiMn_2O_4$ has great advantages, such as lower material cost and low toxicity [4,5]. However, $LiMn_2O_4$ has a problem of severe capacity fading during charge and discharge cycles. Many researchers have suggested and discussed the reason of capacity fading due to some structural degradation with cycling [6–11]. So far, many efforts have been done to improve the electrochemical cycleability of $LiMn_2O_4$ by suppressing severe capacity fading [9–11].

By the way, the Li^+ ion transport processes have been investigated for intercalation materials used in rechargeable lithium batteries. In general, the chemical diffusion coefficient, $\tilde{D}$, is used to describe the complex process of compositional relaxation of active materials. So far, several kinds of measurement methods have been applied to estimate chemical diffusion coefficients of inserted ions in solid electrodes. For example, galvanostatic intermittent titration technique (GITT) [12,13], potentiostatic intermittent titration technique (PITT) [14,15], and electrochemical impedance spectroscopy (EIS) [16–18] have been effectively used. At first, PITT has been frequently used for evaluating the chemical diffusion coefficients. The advantage of this method is that undesirable structural effects on Li^+ ion diffusion coefficient can be avoided when the voltages are controlled to keep a single phase of active materials and to suppress a large compositional change. EIS used for the same purpose with PITT has the same advantages that the diffusion coefficients can be obtained under more equilibrium conditions compared with other methods.

To evaluate electrochemical properties such as a chemical diffusion coefficient, thin films of active materials have been frequently used to simplify the electrochemical system. By employing the thin-film electrode, one can obtain

* Corresponding author. Tel.: +81 426 77 2828; fax: +81 426 77 2828.
E-mail address: kanamura-kiyoshi@c.metro-u.ac.jp (K. Kanamura).
[1] Present address: Department of Chemistry, University of Waterloo, 200 University Ave. West, Waterloo, Ont., Canada N2L 3G1.

0378-7753/$ – see front matter © 2005 Elsevier B.V. All rights reserved.
doi:10.1016/j.jpowsour.2005.07.050

intrinsic response solely from the electrochemical reaction of the material. In order to prepare thin films, various methods have been already developed and proposed, such as chemical vapour deposition [19], sputtering [20], pulsed laser ablation [21], spray coating [22], and so on. When using these methods, however, there is a difficulty in controlling stoichiometry of thin films. On the other hand, a sol–gel method [23], one of soft solution processes, can be considered as a good candidate for fabrication of thin film electrodes. The sol–gel method is well known as one of promising thin film preparation methods with some advantages, such as low fabrication cost, relatively easy stoichiometry control, a fast deposition rate. This method is also well known as a low temperature synthesis for various ceramics.

We have prepared thin-film electrodes using a sol–gel method for rechargeable lithium batteries [24–27]. Our efforts on the preparation of $Li_4Ti_5O_{12}$, $LiCoO_2$ and $LiMn_2O_4$ thin films on Au substrates were successful by introducing poly(vinylpyrolidone) (PVP) to the sol, which was very effective in preparing crack-free thin films [24,25]. In this study, $LiMn_2O_4$ thin-film electrode was prepared by the PVP sol–gel method, and its electrochemical properties were studied using cyclic voltammetry (CV), EIS, and PITT.

2. Experimental

$LiMn_2O_4$ thin film was prepared on a gold substrate by using a PVP sol–gel coating method according to our previous report [24]. Poly(vinylpyrrolidone) (PVP) powders with average molecular weight of 55,000 were employed. The addition of PVP was very helpful in forming a uniform sol. A molar composition of the sol for the $LiMn_2O_4$ thin film preparation was $Li(CH_3COO):Mn(CH_3COO)_2{\cdot}4H_2O$: PVP:$CH_3COOH$:*i*-$C_3H_7OH$:$H_2O$ = 1:2:2:20:40:40. The sol was also kept at room temperature and served as a coating solution for $LiMn_2O_4$ films. Spin-coating was conducted on Au substrate under a rotation speed of 3000 rpm in order to prepare Li–Mn–O gel film. This gel film was converted to ceramic thin film by heating at temperature of 800 °C in air for 1 h. Both spin coating and heating processes were performed repeatedly, until the film thickness became 1.0 μm. The electrode area was 0.785 cm^2. The obtained thin film was characterized by X-ray diffraction with Cu Kα radiation (Rigaku).

A three-electrode cell was utilized for the electrochemical measurements. Lithium metal wire and foil were used as the reference and the counter electrodes, respectively. The electrolyte was a mixed solvent of ethylene carbonate (EC) and diethyl carbonate (DEC) (1:1 in volume) containing 1 mol dm^{-3} $LiClO_4$. The galvanostatic charge and discharge experiment was conducted with an automatic discharge and charge equipment (HJR-110mSM6, Hokuto Denko Co.). Cut-off voltages were 4.2 and 3.5 V versus Li/Li^+ for charge and discharge processes, respectively. Both EIS and PITT were applied for evaluating the Li^+ ion diffusion coefficient in $LiMn_2O_4$. Electrochemical measurements were performed by using an automatic polarization system (HZ-3000, Hokuto Denko Co.) combined with 5080 frequency response analyzer (NF electronic instruments). Electrochemical impedance spectroscopy (EIS) was carried out at various electrode potentials in the frequency range from 50 kHz to 10 mHz. In order to realize an equilibrium state of the electrochemical cell, EIS was measured after a potentiostatic polarization for 2 h. The EIS data were analyzed using the nonlinear least-squares fitting program ZSimpWin (Echem Software). Potentiostatic current transient experiment was also performed. A potential step of 10 mV width was applied and a current with time was measured. The current decayed according to Li^+ ion diffusion through the electrode film. The potential step was terminated, and then a new potential step was performed when the current became less than 10 nA, which was 1% or less of the maximum current at onset of the potential step. All electrochemical experiments were conducted in an argon-filled glove box at room temperature.

3. Calculation

3.1. Electrochemical impedance spectroscopy

The chemical diffusion coefficients were estimated by using electrochemical impedance spectroscopy. In order to obtain a diffusion coefficient, a modified Randles–Ershler equivalent circuit model was employed in this study. The Warburg coefficient, σ, can be expressed as follows [28],

$$\sigma = \frac{V_M}{\sqrt{2}zFa\tilde{D}^{1/2}}\frac{dE}{dx} \quad (1)$$

where V_M is the molar volume of the $LiMn_2O_4$, dE/dx a slope of electrode potential curve versus x (x in $Li_xMn_2O_4$), z the charge transfer number for lithium intercalation, which is equal to 1, the constant a the surface area of the electrode, and F is the Faraday constant.

The intercalation capacitance C_{int} as a function with dE/dx is expressed as follows [17],

$$\frac{C_{int}}{W_f} = \frac{dQ}{dE} = Q_I\frac{dx}{dE} \quad (2)$$

where W_f is the weight of the film, dQ/dE the differential capacity of the $LiMn_2O_4$ film at each potential, and Q_I is the specific capacity of $LiMn_2O_4$ (here we used the theoretical value as $Q_I = 532.8\ C\,g^{-1}$). In addition,

$$V_M W_f = V_f M_W \quad (3)$$

Here, V_f is the volume of the film (=La, L: thickness of the film), and M_W is the molecular weight of $LiMn_2O_4$ (180.82 g mol^{-1}). Combining Eqs. (1)–(3) yields Eq. (4).

$$\sigma = \frac{Q_I M_W L}{zFC_{int}(2\tilde{D})^{1/2}} \quad (4)$$

3.2. Potentiostatic intermittent titration technique

In PITT, an equation for time transient current $I(t)$ related to concentration gradient at an electrode/electrolyte interface was derived as follow [14],

$$I(t) = \frac{2zFa(C_s - C_0)\tilde{D}}{L}\sum_{n=0}^{\infty}\exp\left(-\frac{(2n+1)^2\pi^2\tilde{D}t}{4L^2}\right) \quad (5)$$

where z is a charge transfer number of electroactive species, which is equal to 1, F the Faraday constant, and a is an electrode surface area. The C_0 and C_s are concentrations of Li^+ ion before and after a potential step, respectively. Finally, a reasonable approximation can be made for the long time region ($t \gg L^2\ \tilde{D}$),

$$I(t) = \frac{2Q\tilde{D}}{L^2}\exp\left(-\frac{\pi^2\tilde{D}t}{4L^2}\right) \quad (6)$$

After each potential step, the charge, Q, can be determined by using a coulometer in an external circuit. A chemical diffusion coefficient, $\tilde{D}$, was calculated from an intercept at $t=0$ or a slope of linear region in plot of $\ln I(t)$ versus t, where

$$\tilde{D} = -\frac{d\ln(I)}{dt}\frac{4L^2}{\pi^2} \quad (7)$$

4. Results and discussion

Charge and discharge test for the $LiMn_2O_4$ film was conducted at a current density of 50 μA cm^{-2}. The discharge capacity of the $LiMn_2O_4$ thin film was 60 μAh cm^{-2}, which was close to the theoretical capacity of 64 μAh cm^{-2} μm^{-1} (148 mAh g^{-1}). Fig. 1 shows the result of charge and discharge cycling tests for the $LiMn_2O_4$ thin-film electrode prepared by the PVP sol–gel method. The capacity loss of the $LiMn_2O_4$ thin film was not significant. This film with the good electrochemical cycleability was used for the study on Li^+ ion diffusion process.

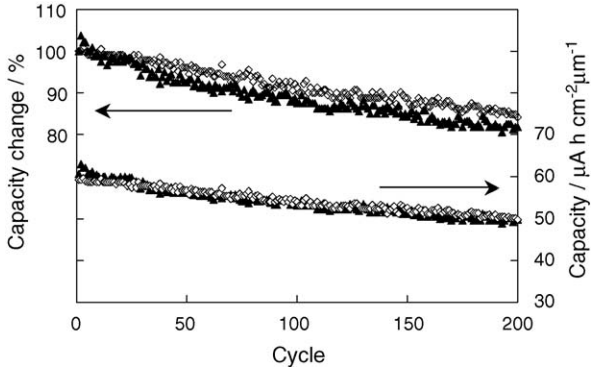

Fig. 1. Charge and discharge capacities of $LiMn_2O_4$ thin film (1.0 μm thick) prepared by PVP sol–gel method. Charge–discharge measurements were carried out at a current density of 50 μA cm^{-2}.

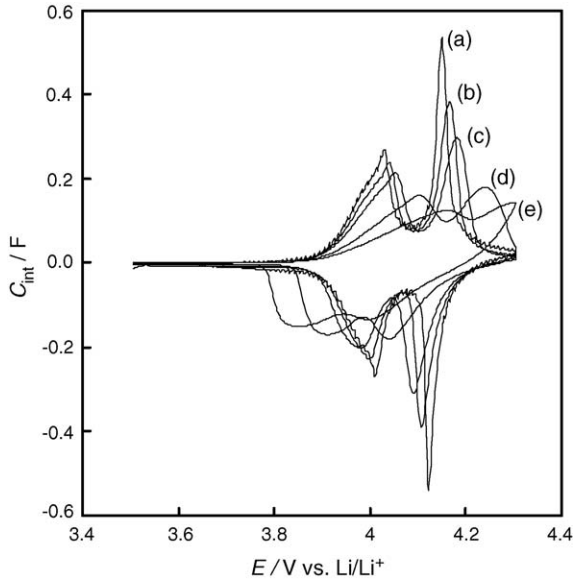

Fig. 2. Cyclic voltammograms of the $LiMn_2O_4$ thin film (1.0 μm thick, surface area: 0.785 cm^2). (a) 0.167 mV s^{-1}, (b) 0.5 mV s^{-1}, (c) 1 mV s^{-1}, (d) 5 mV s^{-1}, and (e) 10 mV s^{-1} in 1 M $LiClO_4$/EC+DEC. $C_{int} = Iv^{-1}$.

Fig. 2 shows the intercalation capacitance, C_{int} obtained from CV. The intercalation capacitance can be obtained from $C_{int} = Iv^{-1}$ (v is the scan rate). At a low scan rate of 0.167 mV s^{-1}, two well-defined reversible peaks were observed at 4.0 and 4.1 V. These peak potentials shifted with increasing the scan rate, reflecting the deviation from equilibrium state at each potential.

EIS was applied for the $LiMn_2O_4$ thin-film electrode. Fig. 3(a) shows a Cole–Cole plot for $LiMn_2O_4$ thin-film electrode measured at 4.00 V. In general, three processes can be distinguished in this diagrams: a slightly depressed semicircle in the high frequency region, a Warburg-type element in the low frequency region, and a steep sloping line at the lowest frequencies. The Warburg region is assigned, naturally, to solid-state diffusion of Li^+ ion into the bulk cathode material, while the steep sloping line reflects a capacitive behavior. This capacitive behavior is due to accumulation of the intercalant (Li^+ ion) into the bulk. All these features of the impedance spectra may be modelled by a modified Randles–Ershler equivalent circuit (Fig. 3 (b)). The same circuit was used previously for $LiMn_2O_4$ single particle electrode [29]. In this model, the electrical components of the surface film likely formed on the particle are disregarded, because no time constant related to this process could be seen in the EIS spectra. R_s is the resistance of the electrolyte, R_{ct} is the charge transfer resistance, W is the Warburg impedance due to the Li^+ ion diffusion in the film, C_{int} is the intercalation capacitance of the $LiMn_2O_4$, and CPE is a constant phase element. The CPE was used instead of double-layer capacitance, to take into account the roughness of the film. Parameters of interest obtained from the simulation of the data according to the equivalent circuit are displayed in Figs. 4–6.

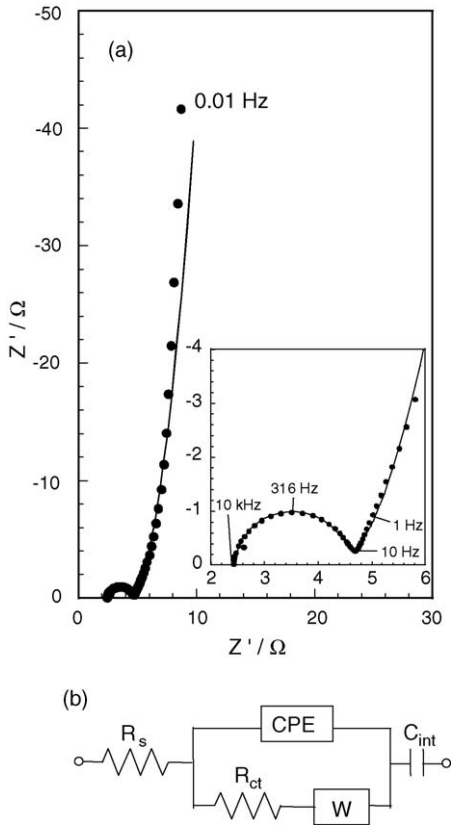

Fig. 3. (a) Cole–Cole plot for the $LiMn_2O_4$ thin film electrode measured at 4.00 V. Solid circle and solid line represent experimental data and simulated curve, respectively. (b) Equivalent circuit model used to model the impedance data.

The charge transfer resistance can be obtained from a diameter of semi-circle appeared at higher frequency region in Cole–Cole plots. Fig. 4 shows the dependence of the charge transfer resistance on the electrode potential. The charge transfer resistance decreased with increasing the electrode potential from 3.8 to 4.0 V, and then increased with increasing the potential from 4.1 to 4.2 V. This tendency is typical for the $LiMn_2O_4$ as reported by other researchers [29–31]. However, the charge transfer resistances were as small as under 10 Ω (7.9 Ω cm^2), which were slightly smaller than reported values [30] probably due to the roughness of the electrode. Fig. 5 shows the intercalation capacitance C_{int} evaluated from EIS. The C_{int} changed, of course, depending on the electrode potential, which was very similar to the C_{int} obtained from CV measured at very low scan rates. Fig. 6 shows the dependence of the Warburg coefficient on the electrode potential. The σ is in unit of Ω s$^{-1/2}$ and inversely proportional to the $\tilde{D}^{1/2}$. Thus, σ can be considered as a resistance barrier for the Li^+ ion diffusion in the solid matrix of the electrode. Sometimes, this kind of information is very useful for qualitatively understanding the diffusion behaviour of intercalated ions in a special condition, e.g. a two-phase reaction in $Li_4Ti_5O_{12}$ [26]. But, in fact, it is not possible to calculate chemical diffusion coefficients precisely in a multi-phase coexistence region where a transient behaviour may be attributed to a phase boundary movement and/or a nucleation of new phase.

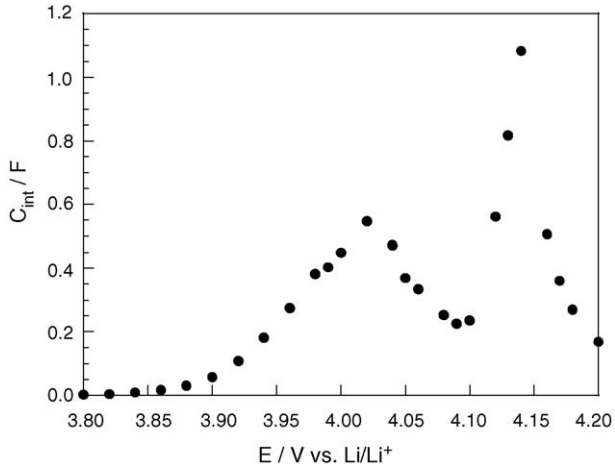

Fig. 5. Plot of the intercalation capacitance (C_{int}) vs. electrode potential.

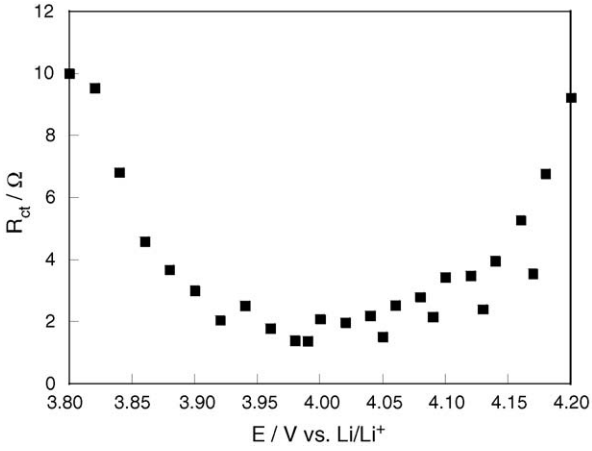

Fig. 4. Plot of the charge transfer resistance (R_{ct}) vs. electrode potential.

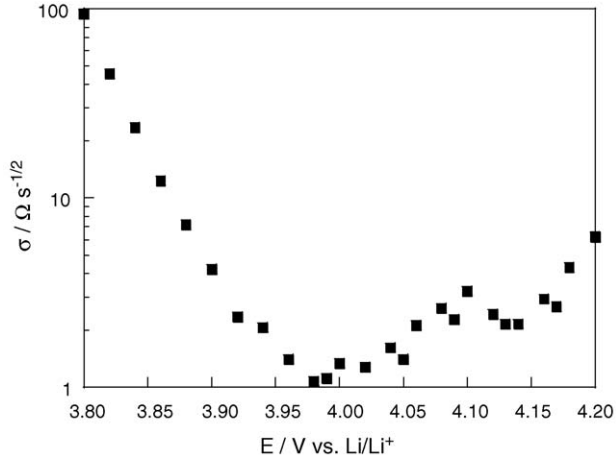

Fig. 6. Plot of the Warburg coefficient (σ) vs. electrode potential.

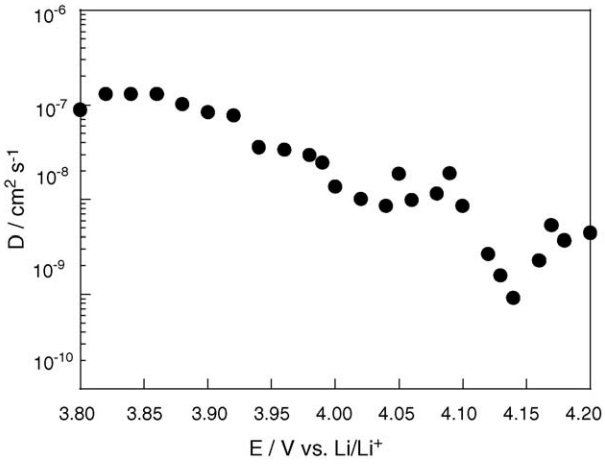

Fig. 7. Plot of the chemical diffusion coefficient (D) vs. electrode potential. D values were calculated from σ and C_{int} using Eq. (4).

In the $Li_{1-x}Mn_2O_4$ system, a two-phase reaction takes place in the range $0.55 < x < 0.9$ [33,34]. The two-phase reaction took place in the potential range from 4.12 to 4.14 V, and the smallest value of the Warburg coefficient was obtained at this potential region, meaning the lowest resistance barrier for Li^+ ion diffusion in this region. The chemical diffusion coefficients were calculated from σ and C_{int} using Eq. (4). Fig. 7 shows the dependence of the diffusion coefficient on the electrode potential. Although the $\tilde{D}$ values in the potential range of 4.12–4.14 V involved the contributions of the two-phase reaction, the apparent chemical diffusion coefficients were estimated. The obtained $\tilde{D}$ values were in the range of 10^{-8} to 10^{-10} $cm^2\,s^{-1}$. This result was comparable with the range of 10^{-8} to 10^{-12} $cm^2\,s^{-1}$ reported in the literatures [13,16,29,31,32].

The chemical diffusion coefficients of Li^+ ion in $LiMn_2O_4$ were also evaluated by PITT. Li^+ ion diffusion in response to a potential step can be described as one-dimensional transport based on Fick's second law. And the Eq. (7) used in this study for calculating the diffusion coefficients. Fig. 8 shows the current-time transient after a potential step 10 mV (from 4.04 to 4.03 V). Straight line for the potential step was obtained

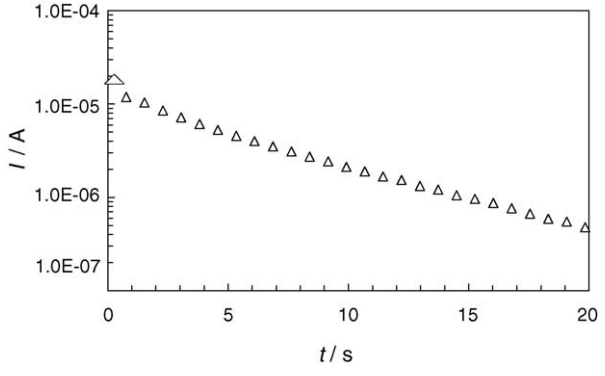

Fig. 8. Typical chronoamperometric curve obtained for the $LiMn_2O_4$ thin-film electrode. The applied potential step used was from 4.04 to 4.03 V.

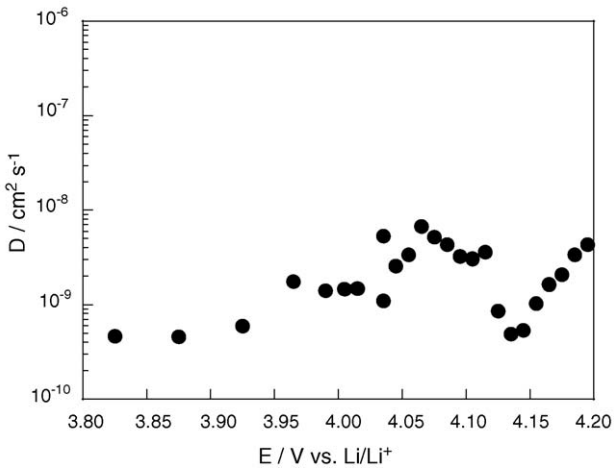

Fig. 9. Plot of the chemical diffusion coefficient (D) vs. electrode potential. D values were evaluated by PITT.

for a long time region. The chemical diffusion coefficients of Li^+ ion evaluated by PITT are shown in Fig. 9. $\tilde{D}$ was ranging from 10^{-8} to 10^{-10} $cm^2\,s^{-1}$, which was well consistent with that obtained from EIS.

5. Conclusions

$LiMn_2O_4$ thin-film electrode was prepared by the PVP sol–gel method. The thickness of the thin film was 1.0 μm. The electrochemical properties of the thin-film electrode were studied using CV, EIS, and PITT. The capacity loss of the electrode was ca. 20% during 200 charge–discharge cycles examined in an electrolyte 1 mol dm^{-3} $LiClO_4$/(ethylene carbonate + diethyl carbonate). The Li^+ ion diffusion in the $LiMn_2O_4$ thin film was investigated by means of PITT and EIS. The chemical diffusion coefficients of the Li^+ ion changed in the range 10^{-8} to 10^{-10} $cm^2\,s^{-1}$ depending on the electrode potential.

References

[1] G. Pisotoia (ed.), Lithium Batteries, New Materials, Developments and Properties, Elsevier, Amsterdam 1994.
[2] B. Scrosati, in: J. Lipkowski, P.N. Ross (Eds.), Electrochemistry of Novel Materials, VCH Publishers, New York, 1993 (Chapter 3).
[3] P.G. Bruce, Chem. Commun. (1997) 1817.
[4] J.M. Tarascon, D. Guyomard, Electrochim. Acta 38 (1993) 1221.
[5] M.M. Thackeray, Prog. Solid-State Chem. 25 (1997) 1.
[6] M.M. Thackeray, Y. Shao-Horn, A.J. Kahaian, K.D. Kepler, E. Skinner, J.T. Vaughey, S.A. Hackney, Electrochem. Solid-State Lett. 1 (1998) 7.
[7] D.H. Jang, S.M. Oh, J. Electrochem. Soc. 144 (1997) 3342.
[8] A. Du Pasquier, A. Blyr, P. Courjal, D. Larcher, G. Amatucci, B. Ger, J.M. Tarascon, J. Electrochem. Soc. 146 (1999) 428.
[9] Y. Xia, M. Yoshio, J. Electrochem. Soc. 143 (1996) 825.
[10] G. Li, H. Ikuta, T. Uchida, M. Wakihara, J. Electrochem. Soc. 143 (1996) 178.

[11] A.D. Robertson, S.H. Lu, W.F. Howard, J. Electrochem. Soc. 144 (1997) 3505.
[12] W. Weppner, R.A. Huggins, J. Electrochem. Soc. 124 (1977) 1569.
[13] M. Wakihara, H. Li Guohua, T. Ikuta, Uchida, Solid-State Ionics 86–88 (1996) 907.
[14] C.J. Wen, B.A. Boukamp, R.A. Huggins, W. Weppner, J. Electrochem. Soc. 126 (1979) 2258.
[15] M.D. Levi, E.A. Levi, D. Aurbach, J. Electroanal. Chem. 421 (1997) 89.
[16] D. Aurbach, M.D. Levi, E. Levi, H. Teller, B. Markovsky, G. Salitra, U. Heider, L. Heider, J. Electrochem. Soc. 145 (1998) 3024.
[17] A. Funabiki, M. Inaba, Z. Ogumi, S. Yuasa, J. Otsuji, A. Tasaka, J. Electrochem. Soc. 145 (1998) 172.
[18] F. Nobili, R. Tossici, R. Marassi, F. Croce, B. Scrosati, J. Phys. Chem. B 106 (2002) 3909.
[19] S.I. Cho, S.G. Yoon, J. Electrochem. Soc. 149 (2002) 1584.
[20] B. Wang, J.B. Bates, F.X. Hart, B.C. Sales, R.A. Zuhr, J.D. Robertson, J. Electrochem. Soc. 143 (1996) 3203.
[21] K.A. Striebel, A. Rougier, C.R. Home, R.P. Reade, E.J. Cairns, J. Electrochem. Soc. 146 (1999) 4339.
[22] T. Uchiyama, M. Nishizawa, T. Itoh, I. Uchida, J. Electrochem. Soc. 147 (2000) 2057.
[23] C.J. Brinker, G.W. Scherer, Sol–Gel Science, Academic Press, Boston, 1990.
[24] Y.H. Rho, K. Kanamura, T. Umegaki, J. Electrochem. Soc. 150 (2003) 107.
[25] Y.H. Rho, K. Kanamura, T. Umegaki, J. Electrochem. Soc. 151 (2004) 106.
[26] Y.H. Rho, K. Kanamura, J. Solid-State Chem. 177 (2004) 2094.
[27] Y.H. Rho, K. Kanamura, J. Electrochem. Soc. 151 (2004) 1406.
[28] C. Ho, I.D. Raistrick, R.A. Huggins, J. Electrochem. Soc. 127 (1980) 343.
[29] K. Dokko, M. Mohamedi, M. Umeda, I. Uchida, J. Electrochem. Soc. 150 (2003) 425.
[30] I. Yamada, T. Abe, Y. Iriyama, Z. Ogumi, Electrochem. Commun. 5 (2003) 502.
[31] M. Mohamedi, D. Takahashi, T. Uchiyama, T. Itoh, M. Nishizawa, I. Uchida, J. Power Sources 93 (2001) 93.
[32] S. Bach, J. Farcy, J.P. Pereira-Ramos, Solid-State Ionics 110 (1998) 193.
[33] T. Ohzuku, M. Kitagawa, T. Hirai, J. Electrochem. Soc. 137 (1990) 769.
[34] T. Eriksson, A.K. Hjelm, G. Lindbergh, T. Gustafsson, J. Electrochem. Soc. 149 (2002) 1164.